RESEARCH PAPER

CrossMark

A novel fluorescent probe for ascorbic acid based on seed-mediated growth of silver nanoparticles quenching of carbon dots fluorescence

Jinshui Liu [1] · Lizhen Wang [1] · Huijuan Bao [1]

Abstract

A novel, economic, and eco-friendly method of detecting ascorbic acid (AA) with excellent sensitivity was developed. The method took advantage of the fluorescence of carbon quantum dots (CDs) decreasing as the AA concentration increased through interactions between AA and Ag(I) in the presence of silver nanoparticle (AgNP) seeds, producing more AgNPs and allowing fluorescence resonance energy transfer between the AgNPs and the CDs. The change in the fluorescence intensity when AA was added was proportional to the AA concentration over the range 0–9.0 μM. The AA detection limit was 0.2 μM. This approach is a new method for determining the concentration of AA.

Keywords Fluorescence · Carbon dots · Silver nanoparticles · Ascorbic acid

Introduction

Ascorbic acid (AA), also called vitamin C, is a water-soluble vitamin that is found at relatively high concentrations in fruits and vegetables. AA is required by humans and other animals for metabolism and is consumed in relatively large amounts [1]. AA plays vital roles in humans and many other animals and can decrease the risk of cardiovascular diseases occurring because it is involved in increasing high-density lipoprotein production, downregulating cholesterol and triglyceride synthesis, and decreasing blood sugar and insulin requirements [2]. AA has antioxidant properties and stabilizes a number of compounds including vitamin E and folic acid. AA improves the absorption of iron by reducing ferric iron into the more absorbable ferrous form. A lack of AA can allow oxidative damage to lipids, DNA, and proteins to occur, so AA

deficiencies have been implicated in many chronic diseases [3]. A fast and accurate method for determining AA will clearly be of great use in the pharmaceutical, clinical, food industry, and environmental analysis fields and also in other fields. Various methods involving spectrophotometry [1], chemiluminescence [4], electrochemistry [5, 6], and other techniques have been used to determine AA. Fluorescence methods offer advantages over other methods, such as offering rapid responses, being very sensitive, and being simple to perform, so have received increasing attention in recent years. Many fluorescent probes, including organic molecules [7], metal nanoclusters [8], and carbon dots [9, 10], have been developed for detecting AA.

Carbon dots (CDs) have attracted much attention because of their fascinating optical properties and prospects for use in efficient optoelectronic devices. CDs have potential for use in biological labeling [11, 12], photocatalysis [13], and fluorescence sensing [14–16]. CDs have low toxicities and high water solubilities and are stable and biocompatible because they have carboxylic acid groups on their exterior surfaces [17]. CDs have been prepared following various synthetic approaches including pyrolysis, electrochemical processes, laser ablation, oxidation processes, and microwave-assisted methods [11–17]. However, most CDs have been prepared using chemical oxidation and exfoliation methods, which have serious disadvantage such as requiring the use of toxic organic solvents and/or strongly basic or acidic media and being time consuming. It is therefore important to develop

✉ Jinshui Liu
jsliu@sina.com

[1] College of Chemistry and Materials Science, Anhui Key Laboratory of Chemo/Biosensing, The Key Laboratory of Functional Molecular Solids, Ministry of Education, Anhui Laboratory of Molecule-Based Materials, Anhui Normal University, Wuhu 241000, China

environmentally benign methods for preparing CDs from raw materials that are widely available [18, 19].

Silver nanoparticles (AgNPs) promise to be useful nanomaterials. AgNPs have been used in many applications because they have remarkable properties including having characteristic high extinction coefficients and exhibiting surface plasmon resonance absorption [20, 21]. AgNPs are also excellent quenchers of various fluorescent probes such as organic dyes and quantum dots [22, 23]. As far as we know, however, CDs have not previously been combined with AgNP seeds and Ag(I) to determine AA. In the study described here, we developed an environmentally benign, simple, cheap, and efficient calcination method for synthesizing CDs from mung bean shells without using any chemical reagents. We then developed a simple, quick, sensitive, and selective method for determining AA using a CD/Ag(I)/AgNP system. The method relied on the CD fluorescence intensity decreasing as the AA concentration increased because of interactions between AA and Ag(I) in the presence of AgNP seeds, producing more AgNPs and allowing fluorescence resonance energy to be transferred between the AgNPs and the CDs, as shown in Scheme 1. To the best of our knowledge, this type of CD has not been used before in a fluorescence probe. We sought to take advantage of the unique features of CDs and AgNPs to design, in a rational way, a new class of fluorescent probe for quickly and sensitively sensing intracellular AA in real samples.

Materials and methods

Chemicals and apparatus

Silver nitrate ($AgNO_3$), potassium nitrate (KNO_3), sodium nitrate ($NaNO_3$), copper nitrate ($Cu(NO_3)_2$), polyvinylpyrrolidone (PVP), sodium borohydride ($NaBH_4$), gallic acid (GA), N-ethylmaleimide (NEM), and catechol were purchased from Sinopharm Chemical Group Co., Ltd. (Shanghai, China). Ascorbic acid (AA) and uric acid (UA) were purchased from Shanghai Bioengineering Co., Ltd. (Shanghai, China).
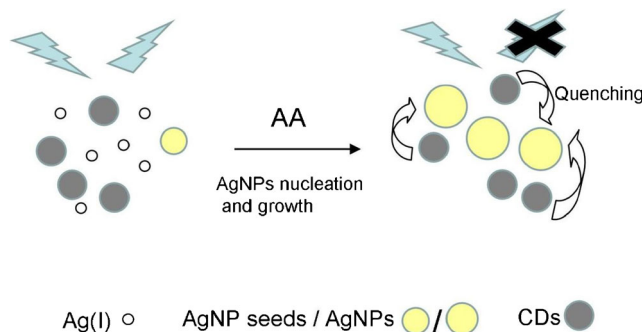
Arginine (Arg), isoleucine (Ile), lysine (Lys), glutathione (GSH), cysteine (Cys), and phenylalanine (Phe) were purchased from Huixing Biochemical Reagent Co., Ltd. (Shanghai, China). Mung bean shell was bought from local agricultural market (Anhui, China). All chemicals used were of analytical reagent grade; experimental water was deionized water.

Fluorescence spectra of all the samples were acquired using an F-4500 instrument (Hitachi High-Technologies), using a 1.0 cm × 1.0 cm quartz cell. The morphologies of the CDs were observed using a Hitachi H-7500 transmission electron microscope (Hitachi High-Technologies Corporation) using an acceleration voltage of 200 kV. UV-vis absorption measurements were made using a U-4100 spectrophotometer (Hitachi High-Technologies Corporation). All the experiments were carried out at room temperature.

Synthesis of CDs

The CDs were synthesized by thermally calcining mung bean shells in a single-step carbonization method. A 9 g aliquot of dry mung bean shells was placed in a crucible, and the crucible was heated to 250 °C for 2 h in a muffle furnace with a nitrogen atmosphere. The black residue was allowed to cool to room temperature, then ground to a powder. The CD synthesis process is shown in Scheme S1 in the Electronic Supplementary Material (ESM). A 0.5-g aliquot of the powder was dispersed, with stirring and ultrasonic, in 50 mL of distilled water to give a CD suspension, which was centrifuged at 8000 rpm for 10 min to remove the larger particles. The supernatant, which contained the CDs, was passed through a 0.22-μm membrane filter and then dialyzed for 10 h using a dialysis membrane with a molecular weight cutoff of 3500 amu. The dialyzed CD suspension was stored at 4 °C until it was used in the experiments described below.

Preparation of AgNP seeds

Each item of glassware was washed with aqua regia (a 3:1 mixture of $HCl_{(conc)}$ and $HNO_{3(conc)}$), rinsed several times with double-distilled water, then dried at 100 °C in an oven. AgNP seeds were prepared by dissolving 0.2 mL of 18 mM $AgNO_3$ and 0.2 mL of 17 mM PVP in 40 mL of deionized water, then 1.2 mL of 10 mM $NaBH_4$ was added dropwise with vigorous stirring. The PVP-stabilized Ag seeds (5–8 nm in diameter) that were produced were kept in the dark at 4 °C until they were used in the experiments described below.

Fluorescence titration experiments

Fluorescence measurements were performed at room temperature using a Hitachi F-4500 fluorescence spectrophotometer using an excitation wavelength of 364 nm and excitation and

Scheme 1 Illustration of the design rationale for the detection of AA using CDs/Ag(I)/AgNP system

emission slit widths of 5 and 10 nm, respectively. A series of test tubes was prepared, each test tube containing a mixture of the CD suspension, 0.1 μM AgNPs, and 30 μM AgNO$_3$ at room temperature. The pH of mixtures was adjusted to 7 by Tris-HNO$_3$ buffer, then the mixtures were allowed to equilibrate at room temperature for 30 min. A different amount of stock AA solution was added to each tube, then deionized water was added to each tube to bring the volume to 5.0 mL. The fluorescence intensity of the mixture in each tube was then measured.

Commercial AA tablet samples were analyzed by adding a tablet to an appropriate volume of deionized water. The fresh human serum was collected from a volunteer of our laboratory and was diluted directly 10 times with buffer before analysis. All experiments were performed in compliance with the relevant laws and institutional guidelines. The solution was passed through a 0.22-mm membrane filter, then the solution was diluted to a specified volume with deionized water and mixed thoroughly before being analyzed. The AA content was determined in AA tablet and human serum samples by the present method and the standard 2,6-dichlorophenolindophenol (DCPIP) method.

Results and discussion

Characterization of the synthesized CDs

Transmission electron microscopy was used to determine the sizes and morphologies of the CDs. The transmission electron microscopy images shown in Fig. 1A indicated that the as-

purified CDs were mostly spherical and monodisperse with diameters of 3–7 nm. These results indicated that the CDs had similar morphological features to CDs produced using chemical synthesis methods [24, 25]. The crystal phases of the CDs were investigated by X-ray diffractometry. The diffraction pattern, shown in ESM Fig. S1, had a broad diffraction peak with a very low intensity centered on 22.14°, indicating that the CDs had amorphous structures. The Raman spectrum of the CDs (ESM Fig. S2) contained a G band at about 1587 cm^{-1}, indicating the presence of intrinsically disordered sp^2 carbon, and a clear D band at around 1360 cm^{-1}, indicating sp^3 carbon [26]. The composition of the CD surfaces and the oxidation states of the elements on the CD surfaces were investigated by X-ray photoelectron spectroscopy. The X-ray photoelectron spectrum shown in Fig. 1B contained three typical peaks, for C 1s at 285.1 eV, for N 1s at 399 eV, and for O 1s at 531 eV. The spectrum also indicated the C, N, and O contents of the CDs. The high-resolution C 1s spectrum shown in Fig. 1C contained three peaks (for C–C at 284.7 eV, for C–O at 286.3 eV, and for C=O at 288.2 eV) [26].

The fluorescence spectrum of the CDs is shown in ESM Fig. S3. Maximum excitation was found at a wavelength of 364 nm, and maximum emission was found at a wavelength of 445 nm. The narrow symmetrical fluorescence peak was consistent with the CD size distribution. The emission spectra were sensitive to the excitation wavelength and the emission peak varied from 425 to 458 nm as the excitation wavelength increased from 320 to 400 nm. It can be seen from Fig. 1D that the emission maximum shifted to a higher wavelength as the excitation wavelength increased. Maximum emission intensity was found at an excitation wavelength of 364 nm. We

Fig. 1 (A) TEM images of the CDs. (B) XPS survey spectra of the CDs. (C) High-resolution XPS spectra of the C 1s of the CDs. (D) Fluorescence emission spectra with different excitation wavelengths
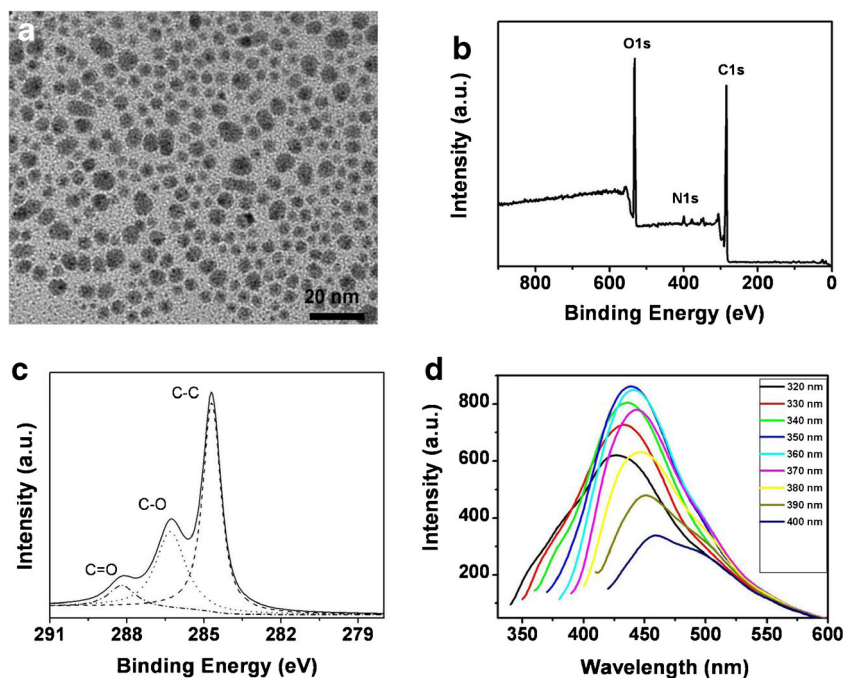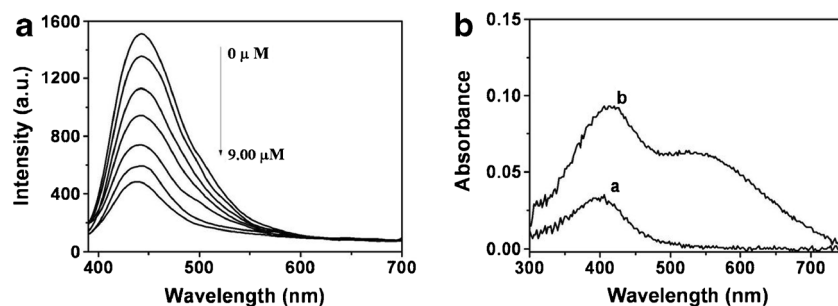
Fig. 2 (A) Fluorescence emission spectra of CDs/Ag(I)/AgNP system and different concentrations of AA (0 μM to 9 μM). (B) UV-vis absorption of (a) Ag(I)/AgNP system and (b) Ag(I)/AgNP system with 4.0 μM AA

therefore concluded that 364 nm was the optimum excitation wavelength for use in the subsequent experiments. This excitation wavelength–dependent fluorescence was attributed to the surface state affecting the CD band gap [27]. The quantum yield of the as-extracted CDs was 18.6%. We concluded that we had successfully synthesized stable and useful CDs.

Fluorescence of the CD/Ag(I)/AgNP system in response to AA

As shown in ESM Fig. S4, the CD solution fluoresced strongly at about 445 nm. Adding 1.0×10^{-7} mol L^{-1} of AgNP seeds and 2.0×10^{-5} mol L^{-1} of Ag(I) decreased the fluorescence intensity slightly because of the CD/Ag(I)/AgNP system forming. Adding a trace of AA quenched the CD/Ag(I)/ AgNP fluorescence, and increasing the AA concentration increased the amount of quenching that occurred, as shown in Fig. 2A. We investigated the effect of the presence of AA on CD fluorescence and found that CD fluorescence was not affected by the presence of AA, as shown in ESM Fig. S5. The decrease in fluorescence was therefore only caused by interactions between the Ag(I)/AgNP system and AA. For sensitive detection of AA, the detection conditions were optimized (the pH, incubation time, and temperature) before quantitatively analyzing AA. As shown in the ESM (Figs. S6–S8), taking these results into consideration, the subsequent

fluorescence titration experiments were performed at pH 7.0 using a Tris-HNO$_3$ buffer solution and a contact time of 30 min at room temperature.

Mechanism involved in the fluorescence quenching process

The mechanism involved in fluorescence quenching was investigated by acquiring UV-vis absorbance spectra of a solution of Ag(I)/AgNPs in the absence and presence of AA. The spectrum for the solution containing only Ag(I)/AgNPs (curve "a" in Fig. 2B) contained a weak absorption peak at around 400 nm. This was the characteristic AgNP absorption peak, called the surface plasmon resonance peak [20, 28]. The spectrum for the Ag(I)/AgNP system containing a trace of AA (curve "b" in Fig. 2B) contained a strong absorption peak at around 400 nm. AA acted as a reductant, transforming Ag(I) into Ag atoms, and the AgNPs acted as nucleation seeds, and grew as Ag(0) was produced [29–31]. The AgNP sizes increased through the nucleation and growth process, but the number of AgNPs also increased. The surface plasmon resonance intensity therefore increased. The quenching of the fluorescence of fluorescent materials by AgNPs is predominantly caused by fluorescence resonance energy transfer, the inner filter effect, and electron transfer [22]. Fluorescence resonance energy transfer or inner filter effect requires the

Fig. 3 (A) TEM images of AgNP seeds. (B) TEM images of Ag(I)/ AgNP system with AA
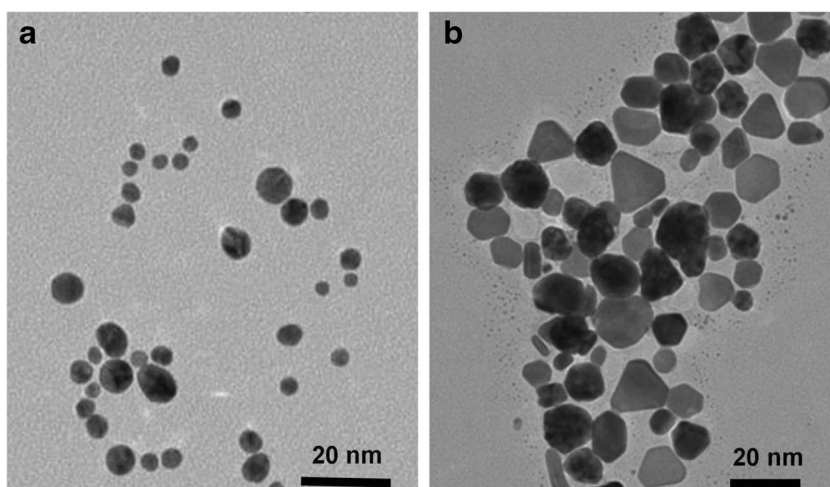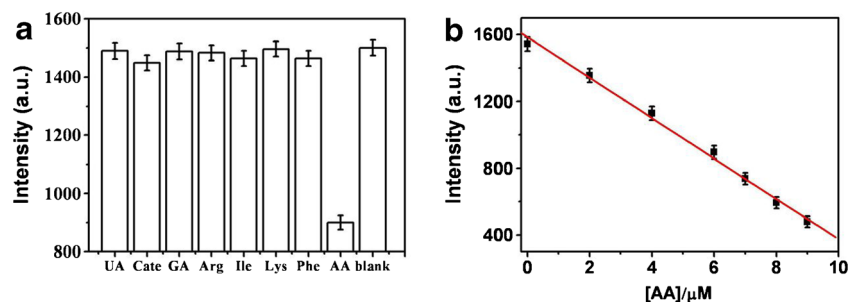
Fig. 4 (**A**) Fluorescence intensities of the CDs/Ag(I)/AgNP system in the presence of AA (6.0 μM) or interfering species (10 μM). (**B**) Linear calibration plot of concentration of AA vs fluorescence intensity

fluorescent materials emission or excitation band to overlap the AgNP surface plasmon resonance band well [32, 33]. The CD emission spectrum (maximum at 445 nm) and excitation spectrum (maximum at 364 nm) overlapped the AgNP absorption spectrum well, as shown in ESM Fig. S9. Transmission electron microscopy images of AgNPs in solutions containing Ag(I)/AgNPs in the absence and presence of AA are shown in Fig. 3. It can be seen from Fig. 3A that the AgNP seeds in the Ag(I)/AgNP system (in the absence of AA) were mostly spherical. The mean diameter of these AgNPs was around 8 nm. Adding AA caused the number of AgNPs and the sizes of the AgNPs to increase, as shown in Fig. 3B. These results supported the conclusion that AA reduced Ag(I) to Ag(0), causing the AgNPs to grow and more AgNPs to be produced.

Selectivity of the method

The selectivity of the sensor for AA was evaluated by determining how various potentially interfering substances affected the fluorescence intensity. The potentially interfering substances that were tested were biomolecules that are commonly found in the environment. These were uric acid, catechol, gallic acid, arginine, isoleucine, lysine, phenylalanine, glutathione, and cysteine. Although glutathione and cysteine could cause detectable responses, N-ethylmaleimide (NEM), a kind of masking agent for thiol group in glutathione and cysteine, could eliminate their interference effectively whereas no effect on the activity of AA [1, 34]. As shown in Fig. 4A, fluorescence quenching was decreased most by AA, and the potentially interfering substances changed the fluorescence quenching efficiency very little. These results indicated that the probe is outstandingly specific and selective for AA and

that nontarget substances do not interfere with the determination of AA using the probe.

Determining AA in samples

The CD/Ag(I)/AgNP system was used to determine the AA concentration in standards containing AA at concentrations between 0 and 9 μM using the optimum conditions. As can be seen from Fig. 4B, a good linear relationship ($R = 0.997$) was found between the fluorescence intensity and the AA concentration in the range 0–9 μM. The equation for the line of best fit for the relationship between the fluorescence intensity (F) and AA concentration (C) was $F = 1583.6 - 121\,C$. The limit of detection (defined as the concentration giving a signal-to-noise ratio of 3) for AA was 0.2 μM. These results indicated that the fluorescence method was comparable to or better than previously described methods for determining AA in terms of the limit of detection, as shown in ESM Table S1 [2, 7, 8, 24, 35–40]. The CD/Ag(I)/AgNP system has many attractive features, including being relatively environmentally benign, being very sensitive to AA, offering good selectivity for AA, being very simple to use, and offering good reproducibility.

We investigated the practicality of the system for determining AA in real samples by analyzing AA tablet and human serum samples by the present method and the standard DCPIP method [41]. NEM (100 μM) was first added to the human serum sample to eliminate the interference from glutathione and cysteine. As shown in Table 1, the analytical results by the proposed method were in good agreement with those by the well-established DCPIP method, and the recoveries of added AA in the samples ranged from 94 to 97%. These demonstrated the method can be used to accurately and reliably determine AA in real samples.

Conclusions

We successfully synthesized fluorescent CDs from mung bean shells using a one-step pyrolytic method. We used the CDs in a CD/Ag(I)/AgNP system to determine AA. The method relies on the CD fluorescence intensity decreasing as the AA concentration increases because of interactions between AA

Table 1 Analytical results of AA in real samples ($n = 3$)

Samples	Present method (μM)	DCPIP method (μM)	Added (μM)	Recovery (%)
AA tablet	3.46 ± 0.14	3.53 ± 0.09	2.0	97 ± 4
Human serum	7.11 ± 0.35	7.28 ± 0.15	2.0	94 ± 5

and Ag(I) in the presence of AgNP seeds. The AA reduces Ag(I) to Ag(0), increasing the number of AgNPs and the sizes of the AgNPs. Fluorescence resonance energy transfer between the AgNPs and the CDs occurs, and the CD fluorescence is quenched more as the AgNPs increase in size and number because of Ag(I) ions being reduced to Ag(0). The CD/Ag(I)/AgNP system fluorescence intensity gradually decreased as the AA concentration increased, and AA could be determined using the system with a detection limit of 0.2 μM, which is comparable to or better than previously described methods for determining AA in terms of the limit of detection. The displayed strategy is economically friendly and provides a simple "mix-and-detect" protocol, without the need of tedious structural modification of the CDs. Notably, this platform is much more environmentally friendly as it relieves the involvement of hazarders reagents in the operation process. We expect that more methods for determining analytes using highly sensitive optical biosensor systems like this, based on fluorescence quenching and metal nanoparticle growth, will be developed in the future.

Compliance with ethical standards

Conflict of interest The authors declare that they have no competing interests.

Ethics approval and consent to participate This study was conducted in accordance with the principles of the Declaration of Helsinki and was approved by the Ethical Committee of the Hospital of Anhui Normal University. All blood samples were from healthy persons with their informed consent.

Human and animal rights No violation of human or animal rights occurred during this investigation.

References

1. Ji D, Du Y, Meng H, Zhang L, Huang Z, Hu Y, et al. A novel colorimetric strategy for sensitive and rapid sensing of ascorbic acid using cobalt oxyhydroxide nanoflakes and 3,3′,5,5′-tetramethylbenzidine. Sensors Actuatos B Chem. 2018;256:512–9.

2. Liu H, Na W, Liu Z, Chen X, Su X. A novel turn-on fluorescent strategy for sensing ascorbic acid using graphene quantum dots as fluorescent probe. Biosens Bioelectron. 2017;92:229–33.

3. Rumsey SC, Levine M. Absorption, transport, and disposition of ascorbic acid in humans. J Nutr Biochem. 1998;9(3):116–30.

4. Zhao S, Huang Y, Liu Y-M. Microchip electrophoresis with chemiluminescence detection for assaying ascorbic acid and amino acids in single cells. J Chromatogr A. 2009;1216(39):6746–51.

5. Ergün E, Kart Ş, Zeybek DK, Zeybek B. Simultaneous electrochemical determination of ascorbic acid and uric acid using poly(glyoxal-bis(2-hydroxyanil)) modified glassy carbon electrode. Sensors Actuators B Chem. 2016;224:55–64.

6. Hameed S, Munawar A, Khan WS, Mujahid A, Ihsan A, Rehman A, et al. Assessing manganese nanostructures based carbon nanotubes composite for the highly sensitive determination of vitamin C in pharmaceutical formulation. Biosens Bioelectron. 2017;89:822–8.

7. Abbasi A, Shakir M. An inner filter effect based Schiff base chemosensor for recognition of Cr(VI) and ascorbic acid in water matrices. New J Chem. 2018;42(1):293–300.

8. Wang X, Wu P, Hou X, Lv Y. An ascorbic acid sensor based on protein-modified Au nanoclusters. Analyst. 2013;138(1):229–33.

9. Fong JFY, Chin SF, Ng SM. A unique "turn-on" fluorescence signalling strategy for highly specific detection of ascorbic acid using carbon dots as sensing probe. Biosens Bioelectron. 2016;85:844–52.

10. Huang H, Wang B, Chen M, Liu M, Leng Y, Liu X, et al. Fluorescence turn-on sensing of ascorbic acid and alkaline phosphatase activity based on graphene quantum dots. Sensors Actuators B Chem. 2016;235:356–61.

11. Chen X, Gong F, Cao Z, Zou W, Gu T. Highly cysteine-selective fluorescent nanoprobes based on ultrabright and directly synthesized carbon quantum dots. Anal Bioanal Chem. 2018;410(12):2961–70.

12. Kuo T-R, Sung S-Y, Hsu C-W, Chang C-J, Chiu T-C, Hu C-C. One-pot green hydrothermal synthesis of fluorescent nitrogen-doped carbon nanodots for in vivo bioimaging. Anal Bioanal Chem. 2015;408(1):77–82.

13. Li H, Liu R, Liu Y, Huang H, Yu H, Ming H, et al. Carbon quantum dots/Cu2O composites with protruding nanostructures and their highly efficient (near) infrared photocatalytic behavior. J Mater Chem. 2012;22(34):17470.

14. Omer KM. Highly passivated phosphorous and nitrogen co-doped carbon quantum dots and fluorometric assay for detection of copper ions. Anal Bioanal Chem. 2018;410(24):6331–6.

15. Gao L, Ju L, Cui H. Chemiluminescent and fluorescent dual-signal graphene quantum dots and their application in pesticide sensing arrays. J Mater Chem C. 2017;5(31):7753–8.

16. Llorent-Martínez EJ, Durán GM, Ríos Á, Ruiz-Medina A. Graphene quantum dots–terbium ions as novel sensitive and selective time-resolved luminescent probes. Anal Bioanal Chem. 2017;410(2):391–8.

17. Lim SY, Shen W, Gao Z. Carbon quantum dots and their applications. Chem Soc Rev. 2015;44(1):362–81.

18. Chaudhary S, Kumar S, Kaur B, Mehta SK. Potential prospects for carbon dots as a fluorescence sensing probe for metal ions. RSC Adv. 2016;6(93):90526–36.

19. Fu H, Ji Z, Chen X, Cheng A, Liu S, Gong P, et al. A versatile ratiometric nanosensing approach for sensitive and accurate detection of Hg2+ and biological thiols based on new fluorescent carbon quantum dots. Anal Bioanal Chem. 2017;409(9):2373–82.

20. Bhattacharjee Y, Chakraborty A. Label-free cysteamine-capped silver nanoparticle-based colorimetric assay for Hg(II) detection in water with subnanomolar exactitude. ACS Sustain Chem Eng. 2014;2(9):2149–54.

21. Zhu D, Chao J, Pei H, Zuo X, Huang Q, Wang L, et al. Coordination-mediated programmable assembly of unmodified oligonucleotides on plasmonic silver nanoparticles. ACS Appl Mater Interfaces. 2015;7(20):11047–52.

22. Liu J, Dong ZZ, Yang C, Li G, Wu C, Lee FW, et al. Turn-on luminescent probe for hydrogen peroxide sensing and imaging in living cells based on an iridium(III) complex–silver nanoparticle platform. Sci Rep. 2017;7(1).

23. Li J, Li Y, Shahzad SA, Chen J, Chen Y, Wang Y, et al. Fluorescence turn-on detection of glucose via the Ag nanoparticle mediated release of a perylene probe. Chem Commun. 2015;51(29):6354–6.

24. Gong X, Liu Y, Yang Z, Shuang S, Zhang Z, Dong C. An "on-off-on" fluorescent nanoprobe for recognition of chromium(VI) and ascorbic acid based on phosphorus/nitrogen dual-doped carbon quantum dot. Anal Chim Acta. 2017;968:85–96.

25. Shangguan J, Huang J, He D, He X, Wang K, Ye R, et al. Highly Fe3+−selective fluorescent nanoprobe based on ultrabright N/P codoped carbon dots and its application in biological samples. Anal Chem. 2017;89(14):7477–84.

26. Liang Q, Wang Y, Lin F, Jiang M, Li P, Huang B. A facile microwave-hydrothermal synthesis of fluorescent carbon quantum dots from bamboo tar and their application. Anal Methods. 2017;9(24):3675–81.

27. Gong X, Zhang Q, Gao Y, Shuang S, Choi MMF, Dong C. Phosphorus and nitrogen dual-doped hollow carbon dot as a nanocarrier for doxorubicin delivery and biological imaging. ACS Appl Mater Interfaces. 2016;8(18):11288–97.

28. Parmar AK, Valand NN, Solanki KB, Menon SK. Picric acid capped silver nanoparticles as a probe for colorimetric sensing of creatinine in human blood and cerebrospinal fluid samples. Analyst. 2016;141(4):1488–98.

29. Wang Y, Zhang P, Mao X, Fu W, Liu C. Seed-mediated growth of bimetallic nanoparticles as an effective strategy for sensitive detection of vitamin C. Sensors Actuators B Chem. 2016;231:95–101.

30. Xiong Y, Zhang Y, Rong P, Yang J, Wang W, Liu D. A high-throughput colorimetric assay for glucose detection based on glucose oxidase-catalyzed enlargement of gold nanoparticles. Nanoscale. 2015;7(38):15584–8.

31. Lim SY, Kim JH, Lee JS, Park CB. Gold nanoparticle enlargement coupled with fluorescence quenching for highly sensitive detection of analytes. Langmuir. 2009;25(23):13302–5.

32. Wang L, Liu J, Zhou Z, Xu M, Wang B. Convenient fluorescence detection of Cr(iii) in aqueous solution based on the gold nanoparticle mediated release of the acridine orange probe. Anal Methods. 2017;9(11):1786–91.

33. Mao M, Tian T, He Y, Ge Y, Zhou J, Song G. Inner filter effect based fluorometric determination of the activity of alkaline phosphatase by using carbon dots codoped with boron and nitrogen. Microchim Acta. 2017;185(1).

34. Hu Y, Zhang L, Geng X, Ge J, Liu H, Li Z. A rapid and sensitive turn-on fluorescent probe for ascorbic acid detection based on carbon dots–MnO2 nanocomposites. Anal Methods. 2017;9(38): 5653–8.

35. Zheng M, Xie Z, Qu D, Li D, Du P, Jing X, et al. On–off–on fluorescent carbon dot nanosensor for recognition of chromium(VI) and ascorbic acid based on the inner filter effect. ACS Appl Mater Interfaces. 2013;5(24):13242–7.

36. Hu L, Deng L, Alsaiari S, Zhang D, Khashab NM. "Light-on" sensing of antioxidants using gold nanoclusters. Anal Chem. 2014;86(10):4989–94.

37. Dãnet AF, Badea M, Aboul-Enein HY. Flow injection system with chemiluminometric detection for enzymatic determination of ascorbic acid. Luminescence. 2000;15(5):305–9.

38. Hu W, Sun D, Ma W. Silver doped poly(l-valine) modified glassy carbon electrode for the simultaneous determination of uric acid, ascorbic acid and dopamine. Electroanalysis. 2010;22(5):584–9.

39. Chen X, Xu Y, Li H, Liu B. A nanoclay-based magnetic/fluorometric bimodal strategy for ascorbic acid detection. Sensors Actuators B Chem. 2017;246:344–51.

40. Li N, Li Y, Han Y, Pan W, Zhang T, Tang B. A highly selective and instantaneous nanoprobe for detection and imaging of ascorbic acid in living cells and in vivo. Anal Chem. 2014;86(8):3924–30.

41. Chauhan N, Narang J, Pundir CS. Fabrication of multiwalled carbon nanotubes/polyaniline modified Au electrode for ascorbic acid determination. Analyst. 2011;136(9):1938.